

¹⁵N NMR Study on Site-Selective Binding of Metal Ions to Guanine Runs in DNA: A Good Correlation with HOMO Distribution

Akimitsu Okamoto, Keiichiro Kanatani, Toshiji Taiji, and Isao Saito*

Department of Synthetic Chemistry and Biological Chemistry, Faculty of Engineering, Kyoto University, and SORST, Japan Science and Technology Corporation, Kyoto 606-8501, Japan

Received July 31, 2002; E-mail: saito@sbchem.kyoto-u.ac.jp

Guanine (G) runs such as GG doublet and GGG triplet in DNA are known to be highly susceptible to electrophilic attack by antitumor drugs and mutagens.^{1,2} G runs are also hot spots for oxidative damage caused by ionizing radiation, oxidizing agents, and photoirradiation with endogenous photosensitizers.^{3,4} The high reactivity of G runs stems from the stacking of electron-rich G bases, which are reflected in their low ionization potentials. Previous results on the reactions of G runs indicate that the reactivity of each G in G runs is not equal and a particular G such as 5' G of GG doublet reacts preferentially.^{2,3,5} To explain such unique selectivity, theoretical studies on G runs have been examined, and the highest occupied molecular orbital (HOMO) distributions of G runs have been calculated at different levels.^{6–8} We reported an attempt for mapping HOMO of G-runs by using Co(II)-mediated G oxidation.⁷ The DNA cleavage data obtained from the oxidation of G runs with Co(II) in the presence of benzoyl peroxide as an oxidant correlated nicely with calculated HOMOs, suggesting that Co(II) interacts more strongly with the G having a larger HOMO, in accordance with the previous ¹H NMR studies on the binding of Co(II) to G-rich oligodeoxynucleotides (ODNs).^{9a} We assumed that the interaction of Co(II) or Mn(II), a soft Lewis acid, with the N7 of a highly electron-rich G base is a HOMO-controlled process.

In the present study we examined the interaction of G runs with paramagnetic metal ions such as Mn(II) and Co(II) by means of ¹⁵N NMR using ODNs containing ¹⁵N-enriched G at N7. As the concentration of Mn(II) was increased, broadening of ¹⁵N signals of the 5'G of GG and the middle G of GGG occurred selectively. These binding selectivities were in good agreement with HOMO distributions in G runs obtained by recent high-level MO calculations.⁸

¹⁵N-enriched G^{10,11} (>98% ¹⁵N) at N7 was incorporated into self-complementary ODN containing G runs (Table 1). The interaction between ODN and paramagnetic metal ion was examined by observing line broadening of ¹⁵N-enriched G-N7.

We monitored the change of ¹⁵N NMR spectra by adding MnCl₂ to a buffer solution of ODNs **GG5'** and **GG3'** containing ¹⁵N-labeled G at the 5'- and 3'-ends, respectively, of GG doublet. Since Mn(II) is a typical relaxation probe with an estimated electronic relaxation time of 10⁻⁸–10⁻⁹ s and gives rise to paramagnetic broadening of a signal of G-N7 in its close vicinity, only line broadening as expressed by line width at half-height was measured as a function of metal concentration.^{9,12} The concentration ratio of metal ion to phosphate, *r* ([metal²⁺]/[phosphate]), was changed up to 5 × 10⁻⁵. In the ¹⁵N NMR of **GG5'**, the chemical shift of the signal of ¹⁵N-enriched G-N7 was almost constant at 234.55 ppm regardless of Mn²⁺ concentration, but the height of the signal gradually decreased, and the line width increased with increasing Mn²⁺ concentration (Figure 1a). The line width at half-height was 8.4 Hz when *r* was 0 and broadened to 14.0 Hz when *r* increased to 5 × 10⁻⁵ (Figure 1c). In contrast, when Mn²⁺ was added to a

Table 1. Self-Complementary Oligonucleotides Used in This Study

ODN	sequences
GG5'	5'-d(GAC ¹⁵ NGGCCGTC)-3'
GG3'	5'-d(GACG ¹⁵ NGCCGTC)-3'
GGG5'	5'-d(GAC ¹⁵ NGGGCCGTC)-3'
GGGm	5'-d(GACG ¹⁵ NGGCCGTC)-3'
GGG3'	5'-d(GACGG ¹⁵ NGCCGTC)-3'

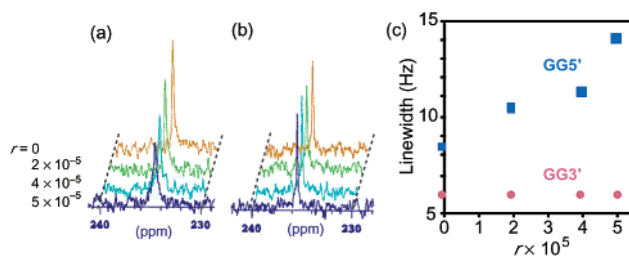


Figure 1. Line width change observed in ¹⁵N NMR of self-complementary duplexes **GG5'** and **GG3'** by changing the concentration ratio, *r* = [Mn²⁺]/[phosphate].¹² (a) **GG5'**, chemical shift = 234.55 ppm. (b) **GG3'**, chemical shift = 235.45 ppm. (c) Correlation of line width with *r*. The estimated errors ±0.4 Hz.

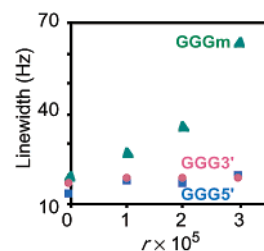


Figure 2. Line width change observed in ¹⁵N NMR of GGG-containing self-complementary duplexes **GGG5'**, **GGGm**, and **GGG3'** by changing the concentration ratio, *r* = [Mn²⁺]/[phosphate]. The estimated errors ±0.8 Hz.

solution of **GG3'**, the signal observed at 235.45 ppm did not show any remarkable change (Figure 1b). In the signal broadening by the interaction with Mn²⁺, a pronounced difference between 5'G and 3'G in GG was clearly observed. The line width change shown in Figure 1c indicates that 5'G was more strongly interactive with Mn²⁺ than 3'G.

We next monitored the change of ¹⁵N NMR spectra by adding MnCl₂ to a solution of ODN containing ¹⁵N-labeled GGG (Figure 2). In the ¹⁵N NMR of **GGG5'**, the signal observed at 234.11 ppm was slightly changed by addition of Mn²⁺. In contrast, the signal for **GGGm** (234.61 ppm) was greatly broadened. The line width at half-height of the signal was 19.2 Hz when *r* was 0, whereas it dramatically increased up to 64.0 Hz when *r* became 3 × 10⁻⁵. On the other hand, when Mn(II) was added to a solution of **GGG3'**, the line broadening of the signal (234.35 ppm) was not observed

Table 2. Increment of Linewidth for GGG-Containing ODNs by Adding Metal Ions

$r = [\text{metal}^{2+}] / [\text{phosphate}]$		increment of line width ^a		
		GGG5'	GGGm	GGG3'
Mn(II)	$r = 0 \rightarrow 3 \times 10^{-5}$	0.45 ± 0.19	1.88 ± 0.22	0.11 ± 0.04
Co(II)	$r = 0 \rightarrow 2 \times 10^{-4}$	0.10 ± 0.09	0.32 ± 0.11	0.05 ± 0.01

^a Increment of line width was given by $\{[\text{line width at } r = 3 \times 10^{-5} \text{ for Mn(II) or at } r = 2 \times 10^{-4} \text{ for Co(II)}] - [\text{line width at } r = 0]\} / [\text{line width at } r = 0]$.

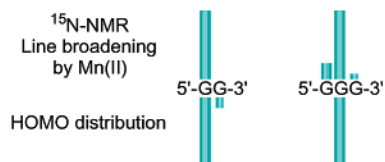


Figure 3. Comparison of line broadening of ^{15}N -labeled G-containing G runs induced by Mn(II) with HOMO distribution obtained by MO calculations. The height of bars in the histogram shows the relative increments of line broadening calculated according to the equation shown in Table 2. HOMO distribution was taken from ref 7 for GG and ref 8 for GGG.

at all. As is clear from Figure 2, a remarkable broadening of the signal by Mn^{2+} was observed only for **GGGm**. Such site-selective line broadening indicates that the middle G of GGG is more strongly interactive with Mn^{2+} than 5'G and 3'G. It is noteworthy that the change of line width of GGG by Mn^{2+} was much larger than that observed for GG. The increment of half-height line width of **GGG5'** was 1.5 times when r changed from 0 to 3×10^{-5} , whereas the line width of **GGGm** expanded up to 2.9 times. These phenomena indicate that GGG is more strongly interactive with Mn^{2+} than GG.

Having established the site-selective interaction of G runs with Mn^{2+} , we examined the interaction with Co(II). The change of ^{15}N NMR signals by adding CoCl_2 to a solution of ODN containing ^{15}N -labeled GGG was monitored. Co(II) has an estimated electronic relaxation time of 10^{-9} – 10^{-10} s, close to that of Mn(II), and was expected to allow the line broadening of the signal of interacting G-N7.⁹ In Table 2, the results on the G-N7 line broadening of ODN containing ^{15}N -labeled GGG are summarized. In ^{15}N NMR spectra of **GGG5'**, a slight line broadening of the signal was observed with addition of Co^{2+} . In contrast, the half-height line width of the ^{15}N NMR signal for **GGGm** increased 32% with increasing Co^{2+} concentration. On the other hand, when Co^{2+} was added to a solution of **GGG3'**, there was not a remarkable change observed in the signal. Addition of Co(II) to a solution of GGG-containing ODN resulted in a middle G-selective line broadening as observed for Mn(II). These data imply that the paramagnetic relaxation by these metal ions is site-selective, suggesting that the middle G is preferential in the metal ion–GGG interaction.

These experimentally observed selectivities matched well with the calculated HOMOs of G runs (Figure 3). We reported earlier that HOMO localizes preferentially at 5'G of GG,^{6,7} and LeBreton and Zhu recently reported that the HOMO almost exclusively resides on the middle G of GGG by calculations of G runs in DNA structures that include the sugar–phosphate backbone.⁸ In addition, the fact that the line broadening for GGG was larger than for GG is also explained in terms of higher HOMO energy level (i.e., lower ionization potential) of GGG than that of GG. The selectivity of

G–metal ion interaction as reported by Sletten and co-workers ($5' \text{GG} \geq \text{GA} > \text{GT} \gg \text{GC}$)⁹ is also consistent with the order of HOMO energies of G sequences ($5' \text{GGG} > \text{GG} > \text{GA} \gg \text{GT}, \text{GC}$).^{3,6,7} The G run–metal ion interaction observed here have also correlated nicely with calculated HOMOs, implying that Mn(II) and Co(II) ions interact more strongly with the G having a larger HOMO. We have reported ab initio MO calculation of molecular electrostatic potentials of GG,⁷ but the difference in the negative electrostatic potentials between the 5'G and the 3'G of GG doublet was not as significant as that observed for the HOMO difference, inconsistent with the experimental results.

Site-selective G–metal ion interaction was demonstrated by ^{15}N NMR of ODNs containing ^{15}N -enriched G in the presence of Mn(II) and Co(II) ions. The selectivity for G–metal ion interaction was in good agreement with calculated HOMO distribution of G runs. Thus, the binding of electron-deficient metal ions to the N7 of electron-rich G is likely a HOMO-controlled process, and as a consequence, the selectivity of the G–metal ion interaction obtained in this ^{15}N NMR study would directly reflect the HOMO distribution of G-containing sequences in DNA. While noncovalent intermolecular forces such as electrostatic interactions, stacking interactions, hydrogen bonding, and hydrophobic effects are well established for DNA–ligand interactions, the interaction of DNA HOMOs with LUMOs of DNA binding molecules could also be another important binding force.^{5,7} The HOMO mapping as described here can visualize the susceptibility of G-containing sequences toward HOMO–LUMO interactions with DNA binding molecules including transition metal ions, thus providing a new tool for probing the heterogeneity of DNA sequences.

Supporting Information Available: Spectral data (PDF). This material is available free of charge via the Internet at <http://pubs.acs.org>.

References

- Warpehoski, M. A.; Hurley, L. H. *Chem. Res. Toxicol.* **1988**, *1*, 315–333.
- Hartley, J. A. In *Molecular Basis of Specificity in Nucleic Acid-Drug Interactions*; Pullman, B., Jortner, J., Eds.; Kluwer Academic Publishers: the Netherlands, 1990; pp 513–530.
- Saito, I.; Nakamura, T.; Nakatani, K.; Yoshioka, Y.; Yamaguchi, K.; Sugiyama, H. *J. Am. Chem. Soc.* **1998**, *120*, 12686–12687.
- (a) Cadet, J.; Delatour, T.; Douki, T.; Gasparutto, D.; Pouget, E.-P.; Ravanat, J.-L.; Sauvaigo, S. *Mutat. Res.* **1999**, *424*, 9–21. (b) Kawanishi, S.; Hiraku, Y.; Oikawa, S. *Mutat. Res.* **2001**, *488*, 65–76.
- Nakatani, K.; Matsuno, T.; Adachi, K.; Hagihara, S.; Saito, I. *J. Am. Chem. Soc.* **2001**, *123*, 5695–5702.
- Sugiyama, H.; Saito, I. *J. Am. Chem. Soc.* **1996**, *118*, 7063–7068.
- Saito, I.; Nakamura, T.; Nakatani, K. *J. Am. Chem. Soc.* **2000**, *122*, 3001–3006.
- Zhu, Q.; LeBreton, P. R. *J. Am. Chem. Soc.* **2000**, *122*, 12824–12834.
- (a) Moldrheim, E.; Andersen, B.; Frøystein, N. Å.; Sletten, E. *Inorg. Chim. Acta* **1998**, *273*, 41–46. (b) Montrel, M.; Chuprina, V. P.; Poltev, V. I.; Nerdal, W.; Sletten, E. *J. Biomol. Struct. Dyn.* **1998**, *16*, 631–637.
- Gaffney, B. L.; Kung, P.-P.; Jones, R. A. *J. Am. Chem. Soc.* **1990**, *112*, 2, 6748–6749.
- Scheller, N.; Sangaiah, R.; Ranasinghe, A.; Amarnath, V.; Gold, A.; Swenberg, J. A. *Chem. Res. Toxicol.* **1995**, *8*, 333–337.
- The DNA samples (4 mM) were dissolved in 0.3 mL of D_2O buffer containing 35 mM sodium phosphate (pD 7.0) and 30 mM NaCl. Aliquots of the salt solutions were added directly into the NMR tube. ^{15}N NMR experiments were performed on Varian Mercury 400 spectrometers at 23.4 °C, operating at 40 MHz for ^{15}N NMR spectroscopy. The number of transients to be acquired was 17000. The vertical scale for signal analyses was fixed at 25000. The chemical shifts were expressed in ppm downfield from liquid ammonia, using 90% formamide in $\text{DMSO}-d_6$ (δ 112.4) as an external standard.

JA0279388